



A review of early twentieth century publications on the subject shows that there was a general tendency to study the lower range of Re. The earliest studies of heat transfer were performed in air [1-3], but these were soon followed by the first attempts to study flows of liquid [4,5]. Two major directions were covered in this stage: that of the average heat transfer from wires, so significant for thermal anemometry, and of the heat transfer from tubes in cross flow.

The second direction of research was closely connected with the progress of boiler design. Along with single cylinders, studies were carried out with arrays, or bundles of cylinders [6].

Recently, the response of the Nusselt number for a circular cylinder to the angle at which the cylinder is yawed relative to crossflow has been studied by Sparrow and Yanez [7]. Their experiments were performed in air and encompassed ten yaw angles in the range between 0 and 60° and the free stream Reynolds number range between 9000 and 70,000. In their study a much denser parameterization than in the past has been represented and supplementary experiments were carried out to investigate the response of the cylinder heat transfer to alterations of the upstream thermal and fluid flow conditions. The same problem has been represented by the heat transfer experiments of refs. [8,9] and the mass transfer experiments of ref. [10]. At a given free stream Reynolds number, these studies yielded different variations of the Nusselt (Sherwood) number with the angle of yaw. In ref. [8], Nu decreased as the cylinder was yawed from cross flow ( $\Theta = 0^\circ$ ) to  $\Theta = 30^\circ$ , then increased slightly in the range  $30 - 50^\circ$ , and decreased thereafter. On the other side, in ref. [9] there was a monotonic decrease of Nu with  $\Theta$ . In ref. [10], Sh actually increased slightly as the yaw ranged from  $\Theta = 0$  to  $15^\circ$  and subsequently decreased with further increases in yaw.

Despite the aforementioned non-monotonic behaviour, it was concluded in refs. [8, 10] that the effect of yaw on the Nusselt number obeyed the so called Independence Principle. According to that principle, the Nusselt number is supposed to be a unique function of the Reynolds number based on the velocity  $U_{\infty} \cos \Theta$ , independent of the yaw angle. Such a representation implies a monotonic decrease of Nu with  $\Theta$  at a fixed free stream Reynolds number, i.e based on  $U_{\infty}$ .

The present experimental work was performed in air and encompassed seven yaw angles in the range between  $\Theta = 0$  and  $28^\circ$  and 6 - 8 values of the free stream Reynolds number between 9000 and 25,000. In addition, supplementary experiments were carried out to study the response of the cylinder heat transfer to alterations of the upstream thermal and fluid flow conditions. As a further supplement to the heat transfer experiments, the pattern of fluid flow adjacent to the cylinder surface was visualized by means of the oil-lampblack technique.

#### EXPERIMENTAL APPARATUS AND PROCEDURE

An experimental test rig was designed and constructed for the planned experiments, see Fig. (1). It consisted of a low-turbulence open circuit wind tunnel of a 30-cm square cross section, in which air from the laboratory room was drawn through the system, by downstream blower (13). The flow rate was controlled by a throttle valve (15). The velocity of the air stream drawn through the system was sensed by the help of Pitot tube (6) and an inclined alcohol manometer (26) at the centers of nine imaginary equal square areas into which its plane was divided, the Pitot tube being situated 50 cm upstream. The air velocity was also measured by the hot-wire probe (5) located 75 cm upstream. The difference in velocity values by the two methods was about  $\pm 1\%$ .

Figure (1) shows the general layout of the experimental apparatus with the associated air supply system and the heating tube. Figure (2) shows a schematic

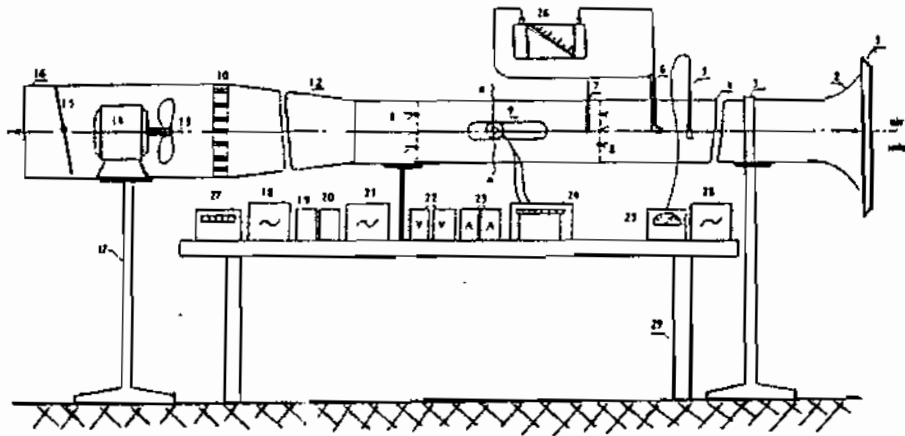


Fig. (1) a) Experimental Test rig.

1- stabilizing plate, 2- inlet collector, 3&17- wind tunnel carriers, 4- stabilizing section, 5- thermoanemometer probe, 6- Pitot tube, 7-thermo- meter, 8- copper-constantan thermocouples, 9- test tube, 10- honeycomb, 11-test section duct, 12-connection section, 13-downstream blower, 14 - -electric motor, 15- throttle value, 16- outlet section, 18- main heater autotransformer, 19-main heater voltmeter, 20- main heater ammeter, 21&28- two autotransformers of guard heaters, 22-two voltmeters guard heaters, 23- two ammeters of guard heaters, 24- temperature recorder, 25- thermoanemometers, 26- inclined tube manometer, 27- digital multimeter, 29-stand table.

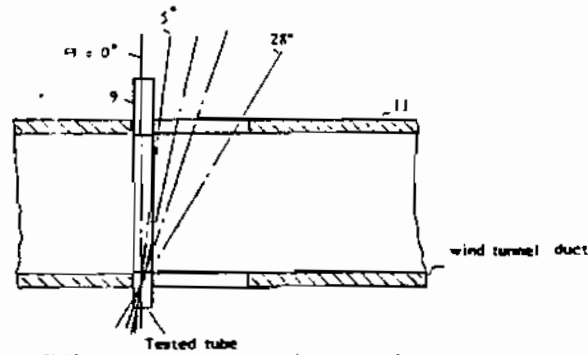


Fig.(1-b) Test section duct plan (sec. a - a).

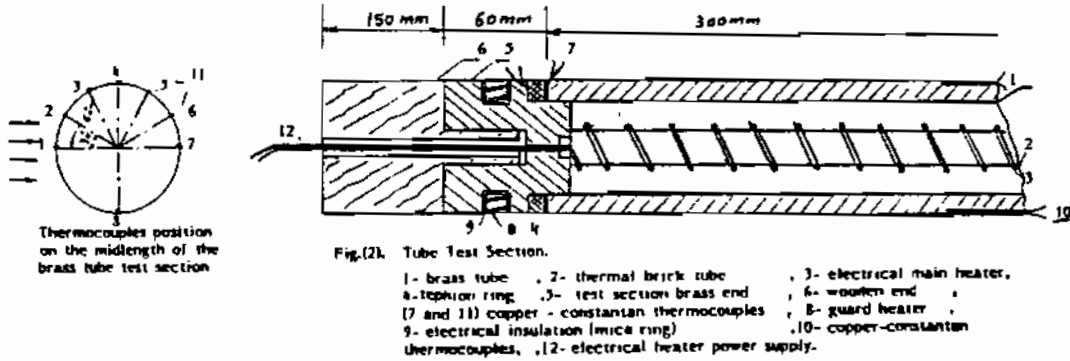
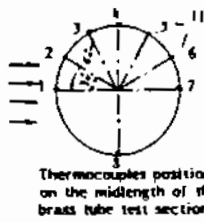


Fig.(2). Tube Test Section.

1- brass tube, 2- thermal brick tube, 3- electrical main heater, 4-topflon ring, 5- test section brass end, 6- wooden end, (7 and 11) copper - constantan thermocouples, 8- guard heater, 9- electrical insulation (mica ring), 10- copper-constantan thermocouples, 12- electrical heater power supply.



Thermocouples position on the midlength of the brass tube test section

diagram of the test tube. A polished brass tube (9) having outer diameter (D) equal to 32 mm, inside diameter (d) equal to 27 mm and 300 mm long is used. On the brass tube test section, there are eight copper-constantan thermocouples (11) distributed as shown in Fig (2-b) at the mid length of the test tube. The copper-constantan thermocouples used are made from 30 gauge wires and are fixed in thin slots (1 mm deep) cut on the outer surface of the tube. Thus the average of eight local temperatures is obtained as follows

$$T_w = [ T_1 + T_2 + T_3 + T_5 + T_6 + T_7 + (T_4 + T_8) / 2 ] / 7 \quad (1)$$

One may observe that the values obtained by the thermocouples of points 4 and 8 should be close equal to each other, because they are located in two symmetrical positions on the test tube. Thus, the mean value of the two readings is used. During this experimental work the difference between  $T_4$  and  $T_8$  was about + 0.025 °C. The tube was heated electrically by means of the main heater (3). This heater consisted of a nickel chromium heating wire wound around a thermal brick tube (2) and situated in the test section brass tube as shown in Fig. (2-a). To prevent the heat loss from the main heater ends two guard heaters (8) were used. The combination of the guard heater is shown in Fig. (2-a). The guard heater is located in electrically insulated groove made on the test section brass end (5). The heat input to each of the main and guard heaters is controlled by using autotransformers (18), (21) and (28) as well as three voltmeters (19) and (22) and three ammeters (20) and (23), see Fig. (1). A teflon ring (4), located in between the two ends of the brass main test tube (1) and the brass end of the test tube (5) of outside diameter 32 mm and inside diameter 27 mm and its length is 5 mm. The whole set is placed in between the two wooden ends (6). For a fixed main heater input, the guard heater input is regulated so as to maintain as small a temperature difference as possible less than 0.2 °C (less than 0.01 mv on the digital multimeter (27), Fig. (1) across the teflon ring (4) thereby ensuring that the heat flow from the test tube ends is negligible. Twelve-junction thermocouple used for this purpose had three junctions on each side of the teflon ring (4). The junctions are located at the midheight of the teflon ring at three locations each of them has 120° apart from the others. These thermocouples are connected to digital multimeter (27) with an accuracy of 0.001mv. Two wooden ends (6) are fixed at the test section ends. the total length of the test section assembly is 700 mm.

The flow air stream temperatures before and after the test tube, and the wind tunnel surface temperature are measured by the set of thermocouples (8) located as shown in Fig. (1). The test tube assembly is supported in the wind tunnel duct as shown in Fig. (1 - b) in which it can be moved to have different yaw angles ( $\theta$ ) is adjusted by rotating the whole test tube around one of the two ends at 0, 5, 10, 15, 20, 25 and 28 deg [see Fig (1 - b) ] .

In order to find the heat lost by radiation ( $q_r$ ) the average value of emissivity of 0.03 for polished brass tube is taken from [11], in which they reported that no significant dependence of emissivity on temperature was observed. The values of  $q_r$  were of order of 0.23 % of the input power to the main heater  $q_{in}$ , neglecting the heat loss by conduction from the ends of the test tube ( $q_{ep}$ ). A steady state was usually achieved after about 3 hours. The average convective heat transfer coefficient was determined from the expression

$$h = q / A ( T_w - T_{\infty} ), \quad Nu = h D / K \quad (2)$$

The probable error in finding the average heat transfer coefficient was estimated to be about + 7 %. The projected area of the test tube on a vertical plane perpendicular to the tunnel axis were estimated by the following correlation

$$A_p = D \times L \cos \theta \quad (3)$$

It is found that the maximum blockage of the wind tunnel free stream cross section area at higher values of  $\theta$  is about 10%. Test and Lessmann [12] have reported that their heat transfer results with and without blockage differ by a maximum of 7%. Therefore, the blockage does not affect the heat transfer results to some extent.

## RESULTS, DISCUSSION AND CONCLUSIONS .

### Heat Transfer Results :

For the determination of the heat transfer coefficients and their correlation with air flow, some quantities were measured for each data run. The power input to the main heater, the heat lost by radiation, the average tube surface temperature, the air flow stream velocity and the free stream temperature were recorded. The heat lost due to imbalance between the main and guard heaters was neglected because the temperature difference on the sides of the teflon rings was kept very small (less than 0.2 °C). Net rate of heat transferred by convection was used to calculate the average heat transfer coefficient from equation (2). The typical deviation of any thermocouple reading from the average wall temperature was 0.25% of  $(T_w - T_\infty)$ . Similarly, the three free stream thermocouples were averaged to obtain  $T_\infty$ , with typical percentage deviations being 0.11% of  $(T_w - T_\infty)$ .

For the Reynolds number, account was taken of the fact that the presence of the cylinder results in the 10% blockage of the cross section of the wind tunnel. The blockage correction for the free stream velocity was based on equation (8a) of Morgan [6] which, when evaluated for the condition of the experiments, yielded

$$U^* = 1.052 \cdot U_\infty \quad (4)$$

Then, the free stream Reynolds number followed as

$$Re = U_\infty^* D / \nu \quad (5)$$

A Reynolds number  $Re_N$  based on the component of the free stream velocity normal to the yawed cylinder is sometimes used as an alternative to the free stream Reynolds number, i.e

$$Re_N = (U_\infty^* \cos \theta) D / \nu = Re \cos \theta \quad (6)$$

The thermophysical properties appearing in equations (2), (5) and (6) were evaluated at a reference temperature  $(T_w + T_\infty) / 2$ .

The parameters varied independently during the course of experiments included the Reynolds number, the angle of yaw and the temperature difference. The Reynolds number was varied from 9000 to 25000, the angle of yaw from 0 to ~30 deg., the main stream velocity from 6 to 12 m/sec. The temperature difference between the test tube surface and the oncoming air ( $\Delta t$ ) was varied from 5 to 60 °C at a given Reynolds number. In all, 177 data points were obtained and in addition, a number of experiments were repeated.

The results in terms of Nusselt number (Nu) versus Reynolds number (Re) for angles of yaw equal to 0, 5, 10, 15, 20, 25 and 28 deg are shown in Figs. (3-9) respectively.

The experiments performed to establish the generality of the results will now

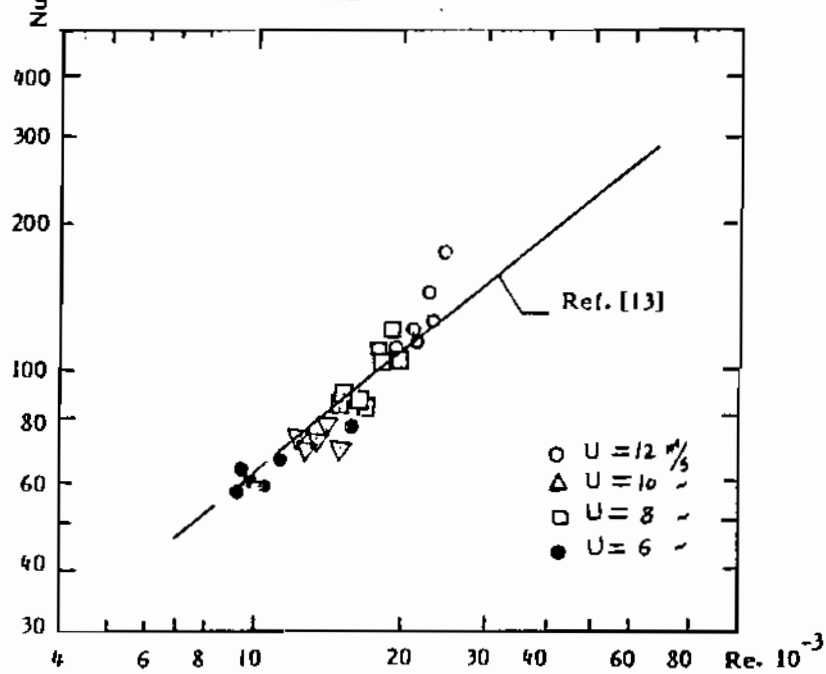


Fig.(3). The Variation of Nusselt number versus free stream Reynolds number at  $\theta = 0^\circ$ .

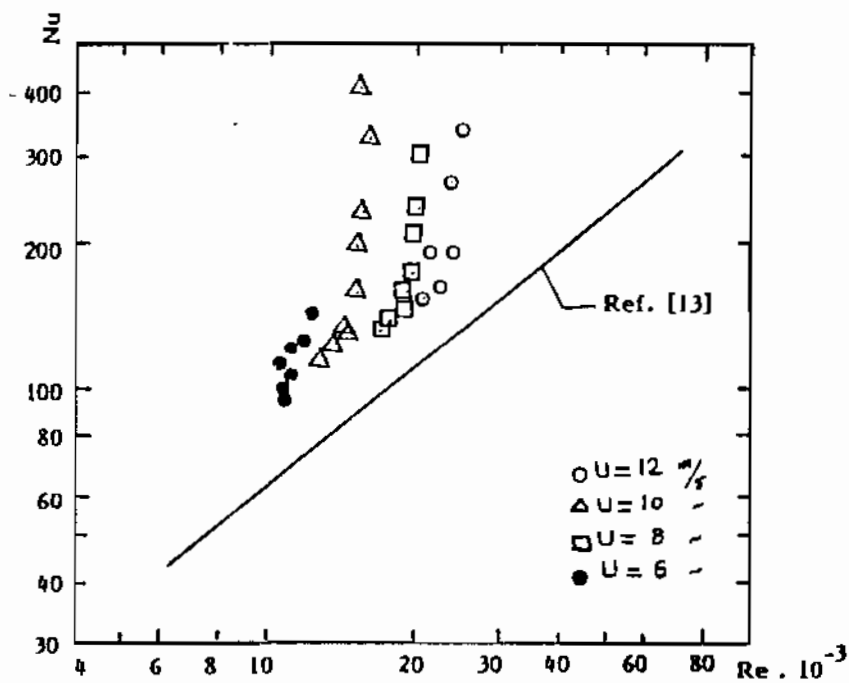


Fig.(4). The Variation of Nusselt number versus free stream Reynolds number at  $\theta = 5^\circ$ .

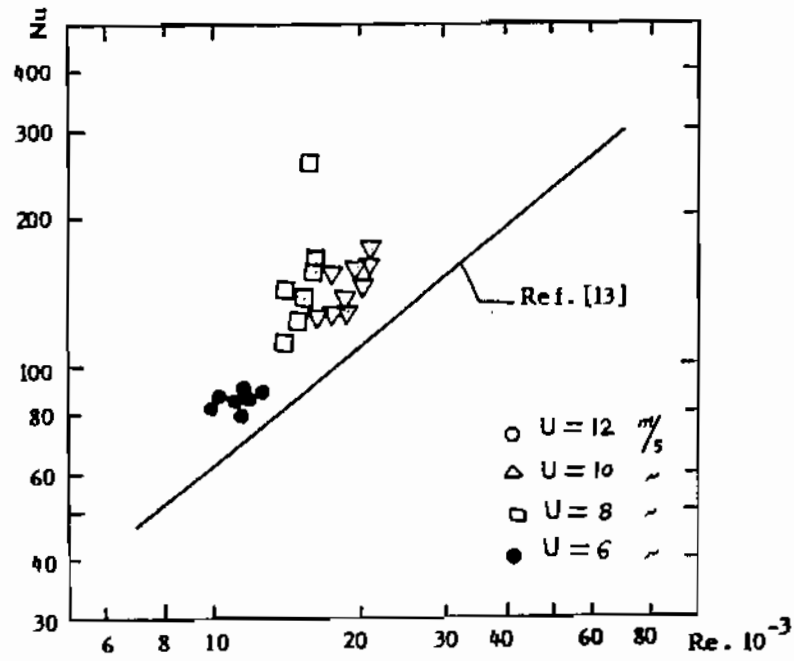


Fig.(5). The Variation of Nusselt number versus free stream Reynolds number at  $\Theta = 10^\circ$

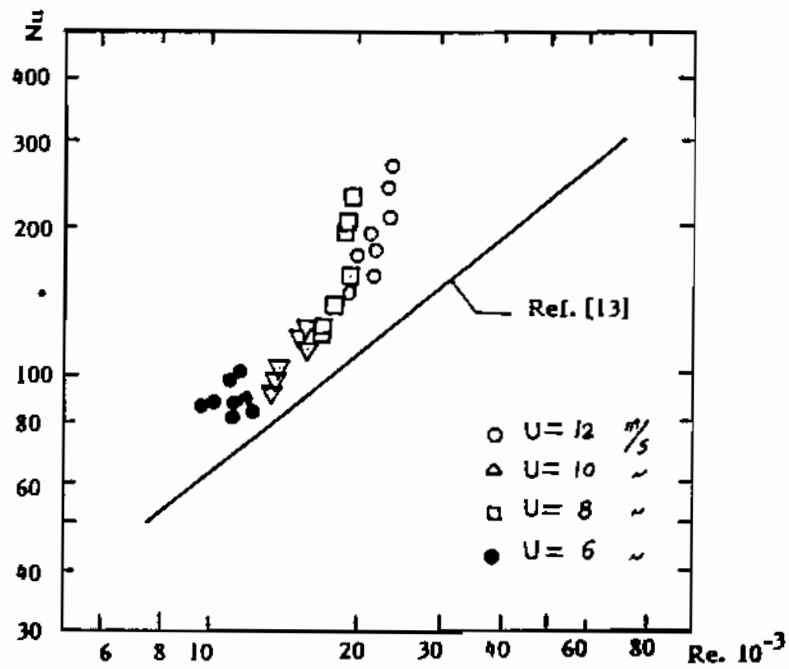


Fig.(6). The Variation of Nusselt number versus free stream Reynolds number at  $\Theta = 15^\circ$

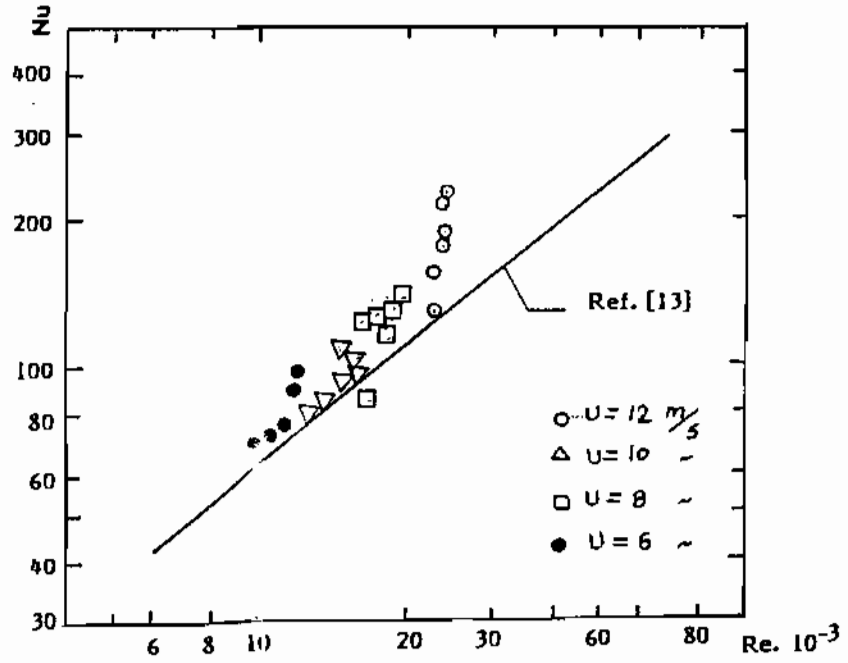


Fig.(7). The Variation of Nusselt number versus free stream Reynolds number at  $\theta = 20^\circ$

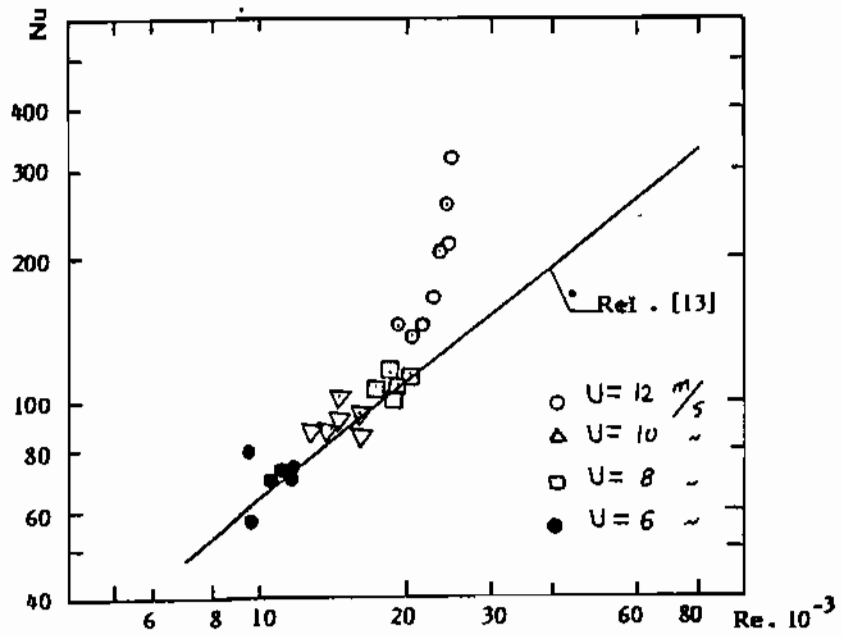
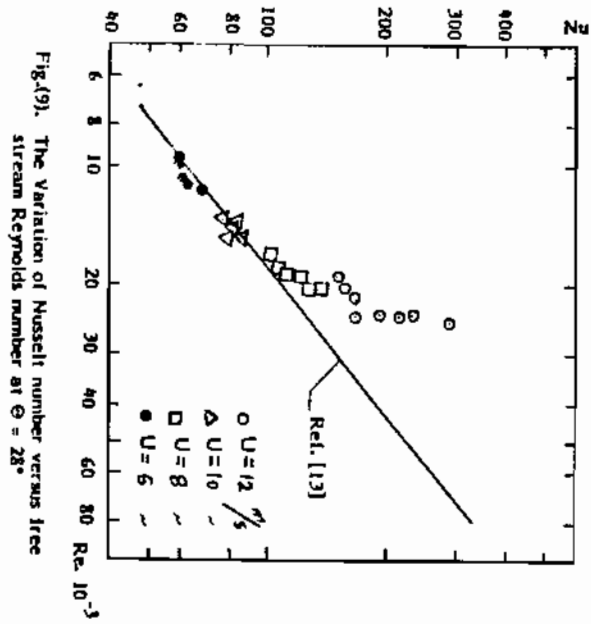
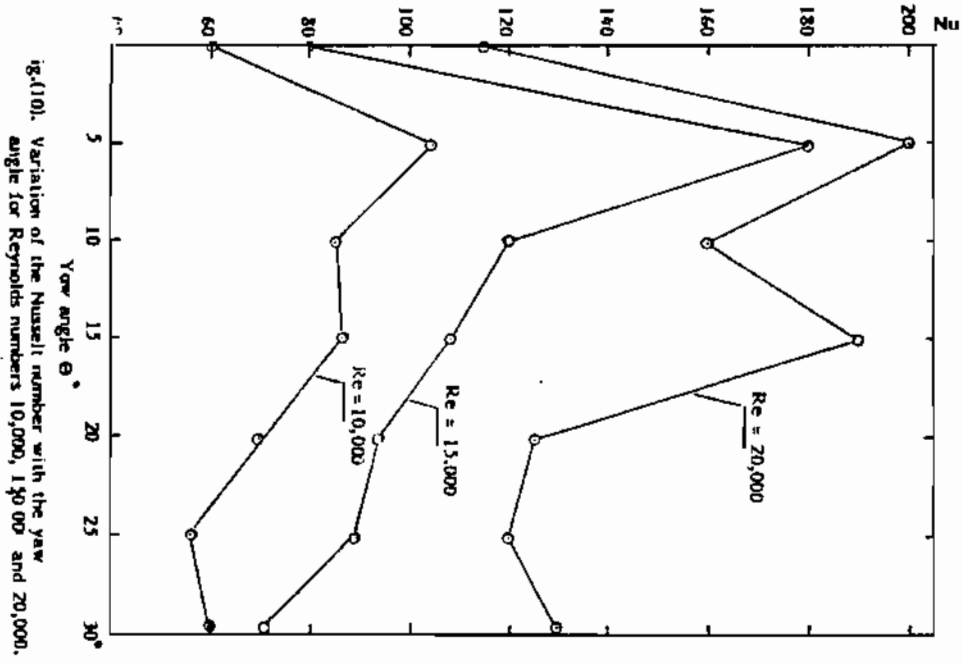


Fig.(8). The Variation of Nusselt number versus free stream Reynolds number at  $\theta = 25^\circ$





be described. The first set of experiments was carried out with the cylinder in cross flow. The cross flow Nusselt numbers are plotted in Fig. (3) as a function of the free stream Reynolds number  $Re$ . Also appearing in the figure is a curve representing the correlation of Zhukauskas (9.2) in Ref. [13]. Inspection of Fig. (3) shows that, for  $\Theta = 0$ , the Nusselt number value increases in general with Reynolds number. The experimental results also agreed within  $\pm 7$  percent with the results obtained from the correlation (9-2) in Ref. [13]. When viewed relative to the spread of the data on which crossflow Nusselt number correlations are based, the level of agreement in evidence in Fig. (3) is highly satisfactory. This agreement lends support to the proper functioning of the apparatus and proper execution of the experiments.

About the response of Nusselt number to yaw angles, one may observe that the Nusselt numbers for each of the seven investigated angles of yaw are plotted as a function of the free stream Reynolds number in Figs (3-9). From an overview of the figures, it is seen that the results for the various yaw angles are not ordered in a regular manner.  $Nu$  increased as the cylinder was yawed from crossflow to  $\Theta = 5^\circ$ , then decreased slightly in the range  $10-15^\circ$ , and decreased thereafter. One may also observe that, in general, Nusselt numbers values increase with the free stream Reynolds number. It is also seen that for Reynolds number values above 20,000 the Nusselt number value is markedly increased as displayed in the Figure. Fig. (10) shows the variation of the Nusselt number with the yaw angle for Reynolds numbers of 10,000, 15,000 and 20,000. The Figure shows that the high  $Nu$  values take place at yaw angle equal to  $5^\circ$ , and then the value decreases gradually with yaw angle. In the case of  $Re = 20,000$ , one may observe that the Nusselt number value increases again at  $\Theta = 15$  and then again it decreases. Fig. (10) is a crossplot of Figs. (3-9).

The complex variation of Nusselt number with the angle of yaw as documented by Fig. (10) is undoubtedly a reflection of changes in the pattern of fluid flow with yaw. An indication of these changes is provided by the flow visualization patterns that will now be presented.

#### Flow Visualization Patterns :

In addition to the heat transfer experiments, flow visualization was performed using the oil-lampblack technique [14]. To facilitate these visualization experiments, the surface of the cylinder was covered with aluminium foil before the mixture of oil and lampblack powder was applied. When the air flow in the wind tunnel was initiated and maintained, the aerodynamic forces acting on the cylinder surface caused the mixture to move and take on a pattern indicative of the pattern of fluid flow adjacent to the cylinder. To obtain a record of the visualization pattern, the aluminium foil was removed from the cylinder surface, laid flat, and photographed. The results is a pattern of streaks which reveal the flow path of the air as it passes over the cylinder surface. In a stagnation region, the oil and lampblack mixture remains as it was initially applied, so that a black region without streaks is indicative of stagnation conditions.

Photographs of the oil-lampblack flow visualization patterns for  $\Theta = 0, 5, 10, 15$  and  $28^\circ$  are presented in Fig. (11). They were selected from a larger collection because they are the sharpest and clearest among those available and because they display noteworthy differences in the pattern of fluid flow.

What is shown in Fig. (11) are photographs of the aluminium foil that had covered the cylinder during a visualization run and that had been removed and laid flat immediately after the run was completed. The photographs were taken with the camera positioned perpendicular to the laid-out contact aluminium foil. The

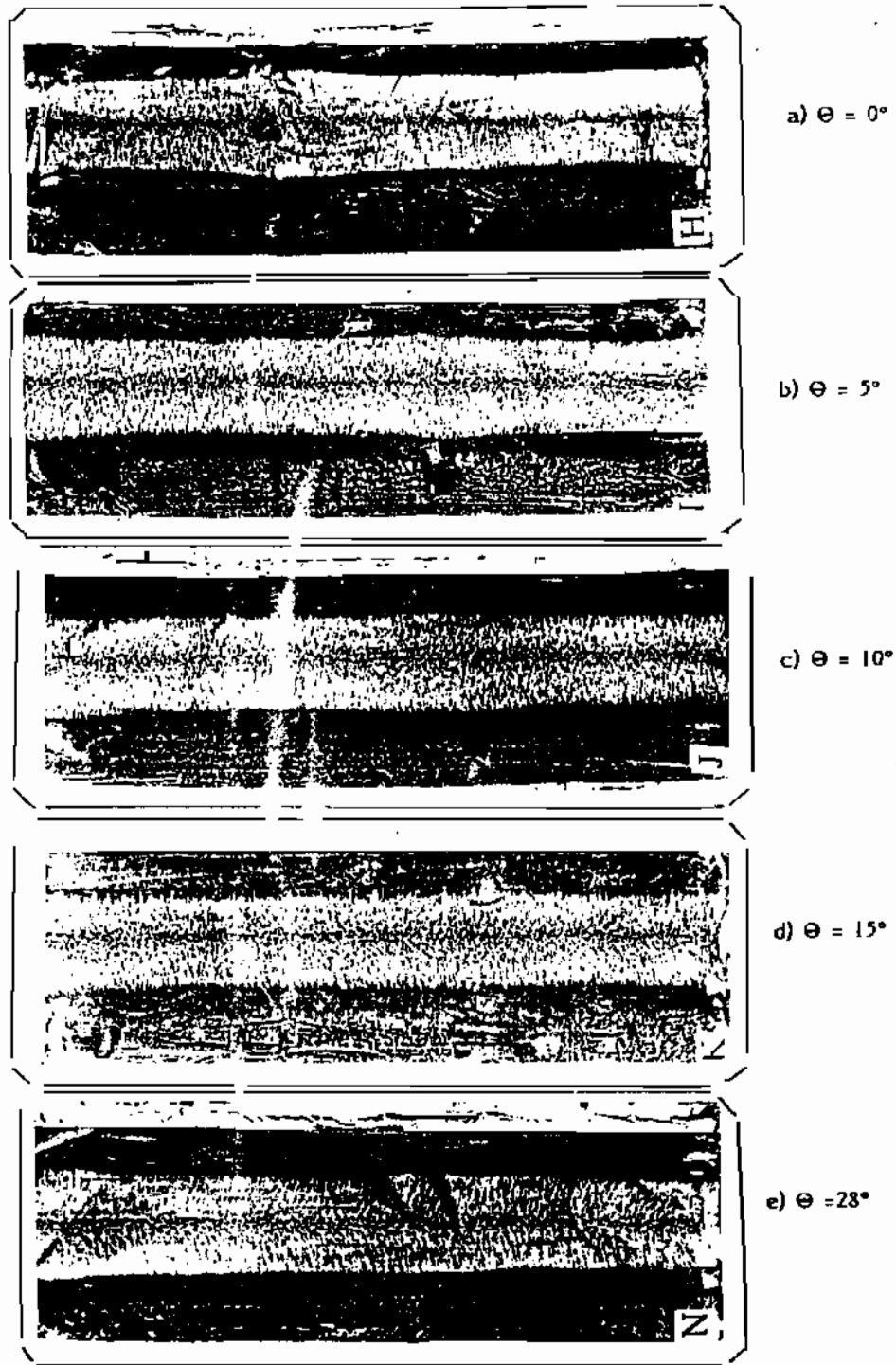


Fig. (11) Flow Visualization Pattern for  $\theta = 0, 5, 10, 15$  and  $28^\circ$ .

views presented in the figure are that of an observer who is situated upstream of the cylinder and is looking downstream.

The main features of the visualization patterns are the central, black horizontal line, the array of the line streaklines which emanate from the black line, and the broad black bands which flank the streak line region. Respectively, these features correspond to the forward stagnation line, the boundary layer region on the forward portion of the cylinder, and the separated region has been masked off because it was marred by finger marks imprinted during the removal of the contact aluminium foil from the cylinder.

The fraying at the ends of the stagnation line reflects the end effects due to the wind tunnel walls. The orientation of the streaklines with respect to the stagnation line is affected by the angle of yaw. For the crossflow case ( $\Theta = 0^\circ$ ), the streaklines are perpendicular to the stagnation line see Fig. (11-a). At the angle of yaw equal to 5, 10, 15 and  $28^\circ$  in Fig. (11-b to 11-e), the angle at which the streaklines emanate from the stagnation lines deviate slightly from the perpendicular. These deviations indicate the presence of a yaw-related axial velocity component. It is also observed that, as the fluid moves around the cylinder, there is a tendency for the direction of the streaklines to approach the perpendicular direction. For the angle of yaw larger than  $\Theta^\circ$ , the streaklines emanating from the stagnation line emerge at an angle considerably different than perpendicular, reflecting the presence of strong axial velocity component. Away from the stagnation lines the streaklines are oriented closer to the perpendicular direction, thereby indicating a less axial velocity component.

#### Correlations:

An attempt is finally made to correlate the data obtained in the present study. Such a correlation is quite useful from a designer's standpoint. The average Nusselt number (Nu) is correlated with the other relevant governing parameters of the test cylinder, namely Reynolds number (Re). So, to provide continuity, a least-squares straight line to the form

$$Nu = C Re^n \quad (7)$$

has been passed through the data for each yaw angle. The numerical values of c and n are listed in Table I

Table. I. The constants c and n for equation (7)

$\Theta$ deg.	0	5	10	15	20	25	28
n	0.80	0.95	0.80	0.80	1.05	1.40	1.40
c	0.038	0.018	0.055	0.057	0.004	0.00015	0.00015

The above equation predicts the values of the data within  $\pm 1\%$ .

Examination of Table I shows that the slope of the Nu-Re variation, as represented by the exponent n, is not very sensitive to the angle of yaw. For the most part, n is in the neighborhood of the crossflow value of 0.8.

The main concluding remark is the Nusselt number for a circular cylinder

does not decrease monotonically as the cylinder is yawed relative to the crossflow orientation. As was discussed in the paper, the investigators of refs. [8-10] have encountered non-monotonic variations of the Nusselt number with yaw angle, but in no case have the variations had the same form. It is believed that the present Nusselt number results are the most generally characterized among those that are available for the yawed cylinder. However the issue is still open since the response of the Nusselt number to free stream turbulence in the presence of yaw has not yet been established.

#### NOMENCLATURE

$A$	tube area, $m^2$
$D$	cylinder outside diameter, $m$
$d$	cylinder inside diameter, $m$
$h$	heat transfer coefficient, $W/m^2\text{ }^\circ\text{C}$
$k$	thermal conductivity, $W/m\text{ }^\circ\text{C}$
$Nu$	Nusselt number, $hD/k$
$q$	rate of heat transfer at cylinder test section, $W$
$Re$	free stream Reynolds number, $U_\infty D/\nu$
$Re_N$	Reynolds number based on $U \cos \theta$
$T_w$	cylinder wall temperature, $^\circ\text{C}$
$T_\infty$	Free stream temperature, $^\circ\text{C}$
$U_\infty$	free stream velocity
$U_\infty^*$	corrected free stream velocity
Greek symbols	
$\theta$	angle of yaw ( $\theta = 0^\circ$ for crossflow)
$\nu$	kinematic viscosity

#### REFERENCES

- 1- Kenelly, A.E., Wright, C.A., and van Bylevel, L.S. "The Convection of Heat from Small Copper Wires." Trans. Am. Inst. Elec. Eng. Vol. 28, PP. 363-393, (1909).
- 2- King, L.W., "On the Convection of Heat from Small Cylinder in a Stream of Fluid." Phil. Trans. R. Soc. AZIA, PP(374-443), (1914).
- 3- Hughes, J.A. "On the Cooling of Cylinders in a Stream of Air." Phil. Mag. Vol. 31, P. 181, (1916).
- 4- Worthington, H.V., and Malone, C.B. "Convection of Heat from Small Wires in Water." J. Franklin Inst. Vol. 184, P.115, (1917).
- 5- Davis, A.H. "Convective Cooling of Wires in Streams of Viscous Liquids." Phil. Mag. Vol. 47, P.282.(1924)
- 6- Zukauskas, A.A. "Heat Transfer from tubes in cross-flow." In Advances in Heat Transfer, New York Academic Press. Vol. 8, PP.93-160, (1972).
- 7- Sparrow, E.M. and Yanez, A.A., "Effect of yaw on forced convection heat transfer from a circular cylinder.", Int. J. Heat Mass Transfer. Vol. 30, No. 3, PP. 427-435, (1987)
- 8- Kraabel, J.S., McMillon, A.A. and Baughn, J.W., "Heat transfer to air from a yawed cylinder.", Int. J. Heat Mass Transfer, Vol.25, PP 409-418, (1982).
- 9- Kazakevitch, F.P. "Effect of the angle of incidence of a gas stream on the heat transfer from a circular cylinder.", Zh. Tekh. Fiz., Vol. 24, PP 1341-1347, (1954).
- 10- Williams, R.E. and Griskey, R.G., "Mass transfer from cylinders at various orientations to flowing gas streams. Can. J. Chem. Engrg, Vol. 53, PP. 500-504, (1975).
- 11- Eckert, E.R.G. and Robert, M. Drake, JR., "Analysis of heat and Mass Transfer.", McGraw-Hill Kogakusha, LTD., (1972).
- 12- Test, F.L., and Lessmann, R.C. "An Experimental study of heat transfer during forced convection over a rectangular body, "ASME Jr. of Heat Transfer, Vol. 102, PP. 146-151, (1980).
- 13- Isachenko, V., Osipova, V. and Sukonek, A., "Heat Transfer.", Mir Publishers Moscow, P. 278, (1969).
- 14- Shalaby, M.A. and Araid, F.F., "Heat transfer and flow visualization of separated reattached air flow over reversed rectangular flat plate", Mansoura Engineering Jr, Vol. 12, No. 1, June (1987).